Airborne campaign results of a compact 2-4um broadband supercontinuum-based spectrometer system for multi-species atmospheric gas analysis at ppm level

L. Balet[a*], S. Chin[a], T. Herr[a], F. Lütolf[a], P. Renevey[a], J. van Zaen[a], S. Dasen[a], S. Droz[a], V. Schaffter[a], J. Gouman[a], G. Buchs[a], F.J.M. Harren[b], A. Khodabakhsh[b], G. Vergara[c], J. Wigg[d], H. Martin[d], L. Huot[e], P.M. Moselund[e], C. Hüglin[f], P. Arsenovic[f], L. Emmenegger[f], and S. Lecomte[a]

[a] CSEM, Laser & Quantum Tech, Systems, 2002 Neuchâtel, Switzerland
[b] Trace gas Research Group, IMM, Radboud University, Nijmegen, the Netherlands
[c] NIT, New Infrared Technologies S.L., Boadilla del Monte, Madrid, 28660 Spain
[d] SenseAir AB, 82060 Delsbo, Sweden
[e] NKT Photonic A/S, DK-3460 Birkerød, Denmark
[f] EMPA, Group for Laser Spectroscopy, 8600 Dübendorf, Switzerland

ABSTRACT

A compact broadband atmospheric gas spectrometer has been developed in the framework of the EU-H2020 FLAIR project. The system is composed of a mid-IR 2-4um broadband supercontinuum source, a temperature controlled 10-meter-long multipass-cell for light-gas interaction, a diffraction grating, and an uncooled PbSe-on-CMOS matrix detector recording absorption spectra. The detection limit has been measured at sub-ppm level on methane under laboratory conditions.

We also present 2 successful field measurement campaigns aboard airborne platforms: a hot-air airship for controlled methane release experiments, and a helicopter tracking ship exhaust fumes abroad the coastline of Denmark, with special emphasis on methane detection.

Keywords: supercontinuum, mid-IR, spectrometer, UAV-compatible, methane, ship fumes

1. INTRODUCTION

FLAIR - FLying ultrA-broadband single-shot InfraRed Sensor (H2020) is a Research and Innovation Action (RIA) funded by the European Union's H2020 program under the Photonics Key Enabling Technologies (KET) topic.

The project seeks to address known challenges in the context of the significant effort that is observed nowadays in active air quality improvement. In order to be successful, these measures need be complemented by air quality monitoring at large scale to ensure compliance with air quality legislation but also to provide information for political decision-making regarding air quality and safety. Large spatial coverage is particularly problematic outside the dense urban network of air quality monitoring stations. FLAIR proposes to close this gap.

The overarching objective of the project is the development of a compact, cost effective and high-performance air sampling sensor based on cutting-edge photonic technology, capable of performing high-specificity and high-sensitivity (ppbv) sensing over large areas by operating it remotely aboard an Unmanned Aerial Vehicle (UAV), commonly known as a drone, or any other suitable platform (e.g., a helicopter).

Operating in the atmospheric windows of 2-5 µm wavelength, the FLAIR sensor aims at detecting minute traces of molecules in complex gas mixtures from their characteristic infrared (IR) absorption fingerprints [1] and provide real time information to the operator of the drone. The whole FLAIR system can operate in remote and/or dangerous areas and outside of established monitoring networks.

*laurent.balet@csem.ch

Photonic Instrumentation Engineering VIII, edited by Yakov Soskind, Lynda E. Busse, Proc. of SPIE
Vol. 11693, 116930Y · © 2021 SPIE · CCC code: 0277-786X/21/$21 · doi: 10.1117/12.2582511

Directly targeted applications include air quality monitoring around industrial infrastructures, maritime and land-based traffic, landfills, and agriculture facilities. The sensor can also be used to coordinate emergency service response in the case of catastrophic events like wildfires, volcanic eruptions, or chemical accidents.

Making the sensor airborne through its integration aboard a flying platform a UAV brings a clear advantage regarding system deployment and pervasive sensing over large areas. Additionally, due to the local character of its sensing operation, the FLAIR sensor can also provide data from inside optically dense clouds and plumes, which are usually not accessible by ground-based laser remote sensing methods.

Photonics technology is a promising approach to the challenge of air quality monitoring, as it can provide, in principle, accurate identification and concentration measurements of specific species in complex environments. Current solutions include several methods for air quality monitoring, among which are mass spectrometry, electronic noses and optical detection. While systems based on mass spectrometry are highly sensitive, they suffer from complexity and high footprint, which hinder integration on a flying platform drone. Electronic noses are cheap but suffer from low accuracy.

Several systems based on light sources operating in the IR range, such as quantum cascade lasers (QCLs), diode lasers, optical parametric oscillators (OPOs) or frequency combs have enabled highly sensitive and selective detection of molecules. Such high-performance tools, however, typically remain confined to academic research laboratories due to their narrow spectral operating window (covering only very few molecules), their operational complexity and their prohibitively high cost. These are the technical challenges FLAIR is addressing.

The FLAIR sensor will generate trace gas absorption spectra from which information on the levels of pollutants can be derived through adequate data processing.

2. SENSOR SUB-SYSTEMS

The FLAIR sensor is composed of several subsystems listed hereafter.

2.1 Supercontinuum light source

In general, supercontiuum laser light [2] can be obtained by broadening the spectrum of a pulsed pump laser in a nonlinear optical fiber. In our case, to reach the mid-IR wavelength range, a fluoride glass fiber ZrF4-BaF2-LaF3-AlF3-NaF (ZBLAN) has been implemented. Supercontinum laser light offers many advantages compared to other types of mid-IR emitters: high brightness (surpassing the synchrotron), coherent emission (allowing for long air – light interaction lengths of several tens of meters), and compactness. [3]

Figure 1. Left: Picture of the first miniature prototype, with dimension 80x120x46 mm^3 and 5V power supply. Right: Picture of the final prototype, with dimension 220x150x55mm^3 and 24V power supply.

The laser system being developed in FLAIR by NKT Photonics is a supercontinuum source initially intended to cover a broad spectral range in the mid-IR region from 2 – 5 µm. A first prototype has been realized, with dimension 80x120x46 mm^3 (Figure 1, left) and running on 5 V power supply. The extremely small dimension of this prototype, compared to commercially available systems, induced stress and twist induced on the fibers. This affected loss and polarization of the signal, as well as strength and lifetime of the splices.

In the optimization stage, a laser producing a narrower spectral band has been designed to cover 2 – 4 µm, specifically aiming to get high spectral density at 3.3 µm for the detection of methane (CH_4), and possibly NO_2, and C_6H_6. This tradeoff had to be made to ensure high spectral density in a ruggedized compact and low power consumption design. The final prototype fits in a 220x150x55mm^3 casing and operates at 24 V (Figure 1, right), where the increased bend radii improved the stability of the system.

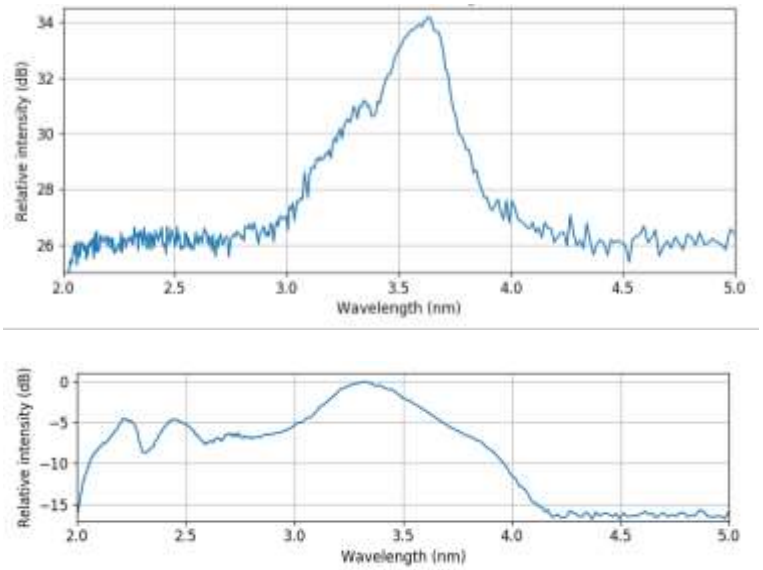

Figure 2. Top: Spectrum of the first miniature prototype. Bottom Spectrum of the final prototype

The spectra of the two light sources are displayed on Figure 2. The final prototype is seeded by an amplified diode laser that produces nanosecond pulses at a repetition rate of 200 kHz and an average power of 1 W. This is an improvement over the initial prototype for a number of reasons. For one, the laser has a higher repetition rate (200 vs 30 kHz), meaning pulse energy is no longer a significant limiting factor in our laser system. This was a constant problem in our previous system, regularly causing failures between the silica-ZBLAN interface. The seed laser is also higher power (1 vs 0.6 W), meaning more power can be transferred to the wavelengths of interest. Table 1 lists the output power of the supercontinuum measured after long pass filters and shows a tenfold improvement in the output power. The laser is also more stable.

Table 1. Long-pass filtered measurements of the laser's output power showing a tenfold improvement in the output power of the supercontinuum.

Cutoff wavelength (nm)	Optimised laser system output power (mW)	Initial laser system output power (mW)
Total	150	15
2500	60	5.0
3000	44	4.1
3500	11	1.8

2.2 PbSe on CMOS camera

The PbSe camera prototype of FLAIR is an adaptation of a Tachyon 16 K manufactured by NIT. Tachyon family are the first uncooled MWIR cameras of the market. The camera heart is a focal plane array of polycrystalline Vapor Phase Deposited (VPD) PbSe deposited directly on the Si-CMOS circuitry, with a resolution of 128x128 pixels and a pixel pitch of 50 μm. It is a breakthrough in the infrared camera domain: VPD PbSe is the first quantum (not thermal) infrared detector monolithically integrable with the Si-CMOS ROIC.

Table 2. FLAIR PbSe camera core main characteristics.

Detector type	VPD PbSe
Array format	128x128
Pixel size (μm)	50x50
Spectral range (μm)	1-5 (AR coating extended)
Integration time (μsec)	10 – 1000 (selectable)
Interface	GigE Vision 2.0 with PoE
Max. frame ratE	2000 fps (interlaced acquisition)
Start up time	< 10 s
Power supply	PoE / non PoE requires 12 VDC)

The spectral response of the PbSe (Figure 2) is well matched to the emission of the supercontinuum, with a maximum near the absorption lines of methane. In addition, since the active aera is protected by a Si window (with high refractive index), NIT applied a specifically designed antireflection coating ensuring more than 90% transmission from 1.5 μm to 4.7 μm.

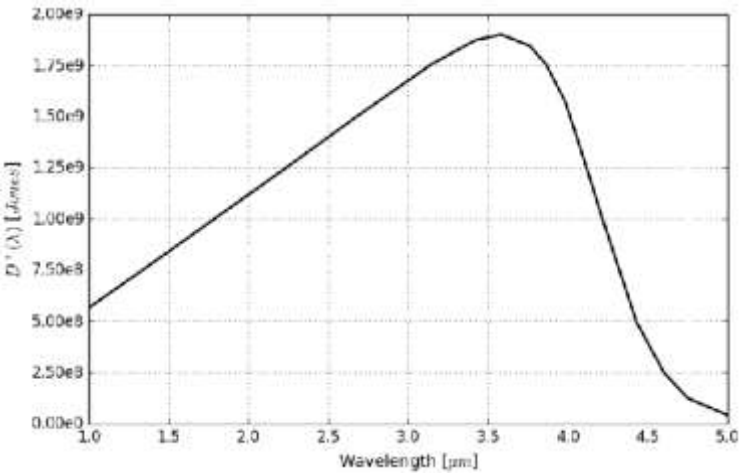

Figure 3. Spectral response from PbSe. [4]

FLAIR application is very demanding in terms of size, weight, power consumption and thermal stability of all components. The PbSe camera, as part of FLAIR instrument, required an envelope which design would help to keep the sensor size, weight and consumption in reasonable values compatible with the FLAIR UAV payload and that would also

be efficient to dissipate heat, keeping the sensor in a narrow range of temperatures. The thermal management of the core of the camera has been specially adapted for FLAIR's application, with an improved heat dissipation.

Table 3. FLAIR PbSe camera prototype characteristics.

Housing	Anodized aluminum
Interfaces	Ethernet RJ45 / M12-C (17 pins)
Dimensions (mm)	66 (L) x 62 (W) x 62 (H)
Optics interface	Cs mount
Weight (g)	397
Active cooling	Optional (when required)
Power consumption (W)	8 (max. frame rate)

However, it has been noticed that during out-of-lab testing, the variation of ambient air temperatures had an impact on the signal of the camera. For this reason, an active temperature stabilization has been implemented with a thermoelectrical cooler (TEC) placed between the camera body and the heat exchanger (see Figure 4). The TEC temperature has been stabilized to 25°C.

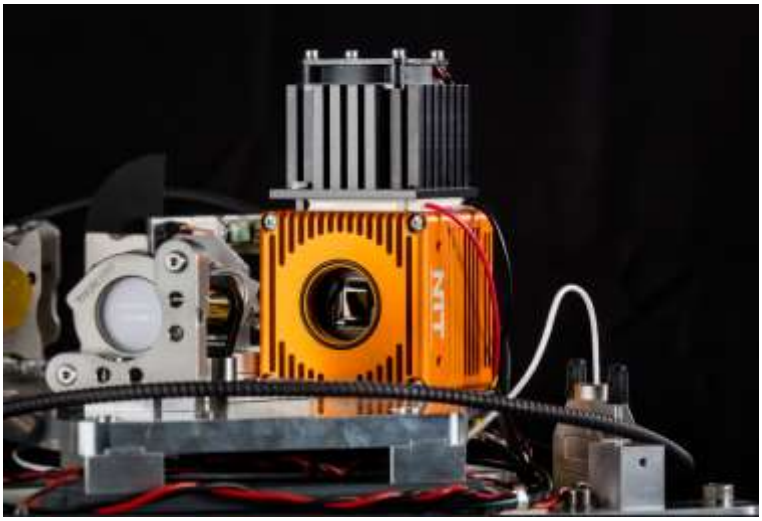

Figure 4. Picture of the PbSe camera as installed on the FLAIR spectrometer prototype. A TEC element placed between the camera and the heat exchanger ensures a good thermal stability in out-of-laboratory operation.

2.3 Multipass cell (MPC)

The role of the multipass cell is to increase the interaction length between the supercontinuum light and the air sample. This, in turn, allows to reduce the detection limit of specific molecules within this air sample. The multipass cell developed for FLAIR by Senseair has a total path length of 12 m. The beam bounces 40 times between 2 mirrors separated by 30 cm. The mirrors are mounted in a cylindrically shaped structures made of low thermal expansion steel.

The mechanical stability of the MPC is of upmost importance. Since it is placed before the spectrometer, any in-operation misalignment, due for example by thermal expansion or vibration, is amplified through the multiple reflection and can impair the functionality of the spectrometer.

The MPC is packaged into a 3D printed enclosure with 2 main functionalities: it serves as temperature stabilized environment for the MPC, like a thermos bottle, and it also manages the input of the sampled gas into the interaction region with light. Hence, the MPC system includes control electronics, ventilation fan, pressure, and temperature sensors for the gas handling, as well as air heaters in the packaging of the absorption cell.

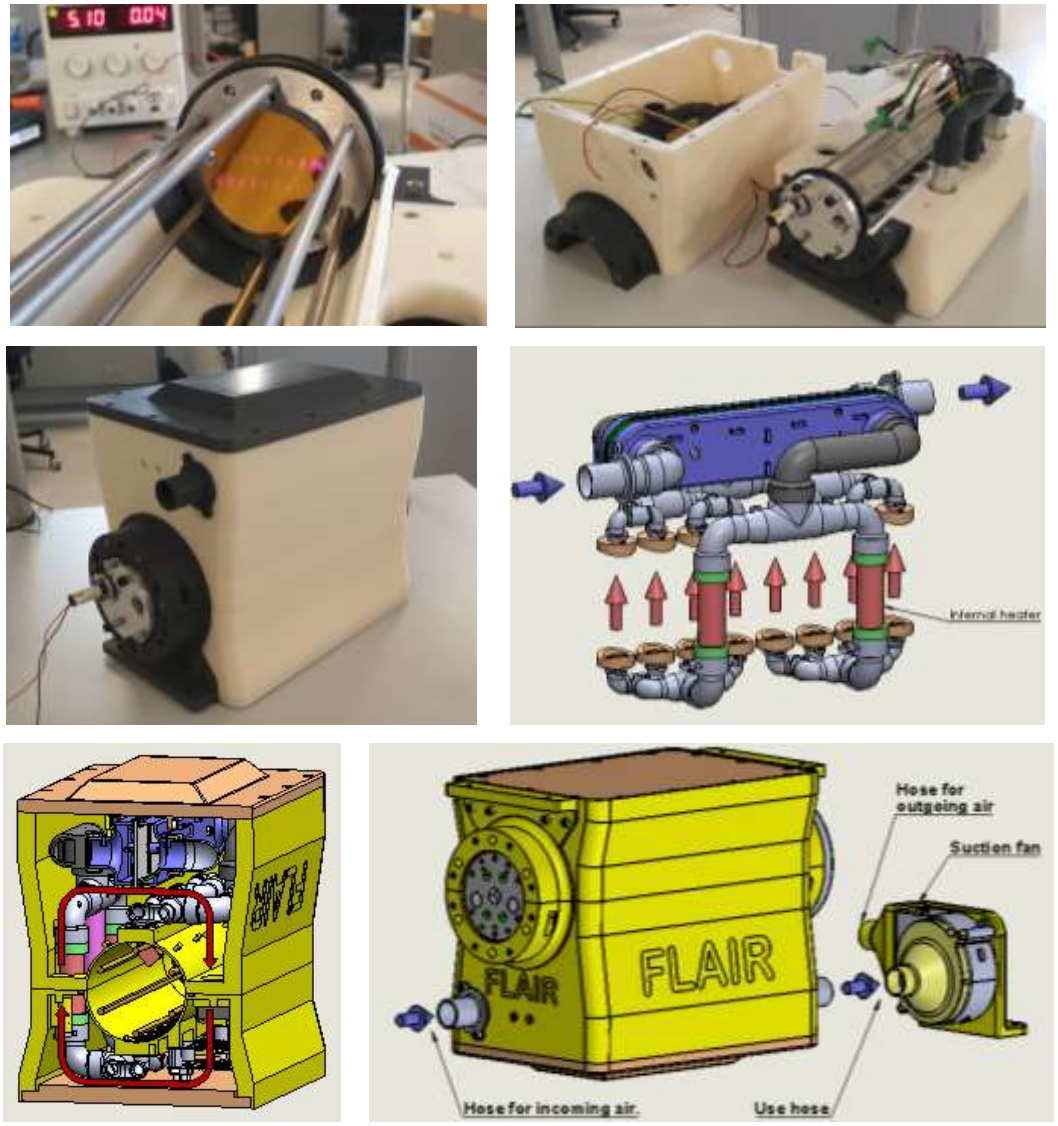

Figure 5. (From top left to bottom right) A. Close view inside the multipass cell during the alignment procedure with a visible 660 nm laser attached to the input port. The multiple reflections are visible on the input mirror. B. The optical part of the multipass cell in the 3D printed enclosure during the assembly procedure. The heater cartridges are visible, as well as some of the electrical cabling. C. Fully assembled multipass cell system. The electronic control card is in the small protuberance on the top. The alignment laser is visible, still attached to the input port. D. Vue of the air management system. Upon entering the air is pre-heated in the blue heat exchanger. It then passes through some manifold, is heated inside the red cartridges, and is forced as a laminar flow through the optical interaction region. It then gives its heat back in the heat exchanger and leaves the MPC system. E. The inside of the MPC is like a thermos enclosure with a thermally controlled air convection system to ensure good thermal stability of the MPC structure. F. Sketch of the fully assembled system. The blower fan can be placed independently before or after the MPC and manages up to 1.2~1.5 liters per second through the MPC.

Figure 5 shows different views of the MPC design. The alignment procedure of the multipass cell is performed with an auxiliary visible 660 nm laser attached to the input port. The cell can be tuned to match different total path length. There is a tradeoff between the lowering of the detection limit due to the longer path, and the decrease of in SNR due to increase reflection losses at the mirror surface.

The optical part of the multipass cell is fitted in the 3D printed enclosure which is designed like a thermos enclosure with a thermally controlled air convection system to ensure good thermal stability of the MPC structure. This 3D printed structure also manages the air circulation within the MPC. A heat exchanger pre-heats the incoming air which then flows through two heater cartridges. The goal is to have a relatively constant air temperature in the sampling chamber, some 3 to 5 °C above the ambient conditions (if the ambient temperature is below 22°C). The air is then forced through adjustable nozzles to ensure a constant air flow across the length of the multipass cell, and a laminar flow condition toward the exit apertures. After exciting the interaction chamber, the air gives some of its heat back in the heat exchanger and is evacuated from the MPC system.

Table 4. FLAIR multipass cell prototype characteristics.

Principle	Confocal spherical mirrors - White cell
Mirror radius of curvature	30,0 cm
Number of passes	4 to 72 (40 for the final prototype)
Optical pass-length	1,2 to 21,6 m (12 m for the final prototype)
Mirror coating	Protected Au
Entrance/exit widows	Edged CaF2
Operating wavelengths	2-12 µm
Interaction chamber volume	~1 Litre
Flow rate	Adjustable, up to 1.5 Litre/second
Built in sensors	2x temperature, 2x relative humidity

Several pumping systems have been evaluated. However, they had not enough flow rate, or were incompatible with the UAV requirement for low weight and low power consumption. Finally, the solution has been the use of a computer blow fan. The flow rate can be adjusted, and once coupled to the MPC, managed to exceed 1L per second.

The MPC is equipped with different sensors and thermal controllers. Besides the temperature sensors controlling the temperature of the thermos enclosure and of the intake air, the interaction region has 2 temperature and relative humidity sensors. All the electrical connectivity is managed by an electronic control card placed within the 3D printed enclosure. It can be controlled by a computer via USB.

2.4 2D spectrometer (laboratory only)

The initial design for the spectrometer part made full use of the 2-dimensional structure of the NIT camera detector. After passing through a gas cell (or the MPC), the supercontinuum light is focused by a cylinder lens on the input port of a virtually imaged phased array (VIPA) that disperses the light in the vertical direction. The light is then dispersed orthogonally by a dispersion grating and imaged onto the NIT camera by an off-axis parabolic (OAP) mirror. The principle is illustrated on Figure 6. [5]

Figure 7 shows the resulting image acquired by the NIT camera, with a 10 cm long reference cell filled with 0.1 atm N_2O gas. The left side shows an average of 1000 images acquired at 1000 fps. The structures are barely visible. We decided to implement a lock-in detection scheme (113 Hz), with a chopper wheel placed on the path of the SC light in front of the reference cell. The image on the right side shows the result of the lock-in demodulation on 1000 frames acquired at 1000 fps. A structure is now clearly visible, with “almost vertical” lines spanning across the camera. Some dark spost are visible. They correspond to wavelength where the light has been absorbed by the gas. To read the spectrum, one must

follow those line (bottom to top), then jumping to the next line (left to right). By concatenating them, one obtains a linear spectrum. To avoid that higher order of the VIPA interfere with the acquired spectrum, a 3.7 µm – 4.5µm bandpass filter has been placed in front of the gas cell.

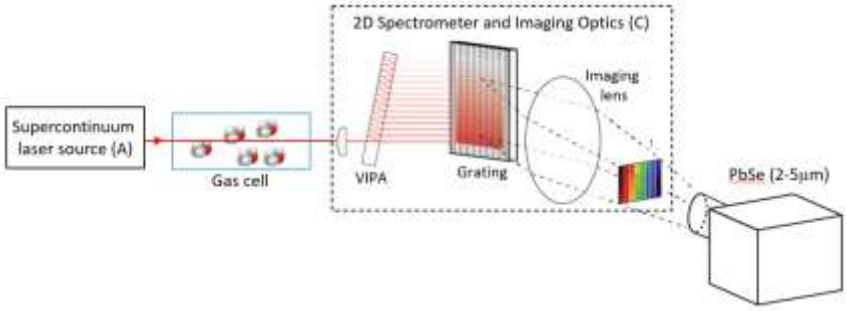

Figure 6. Working principle of the 2D spectrometer design initially foreseen for FLAIR. The imaging lens has been replaced by an OAP mirror.

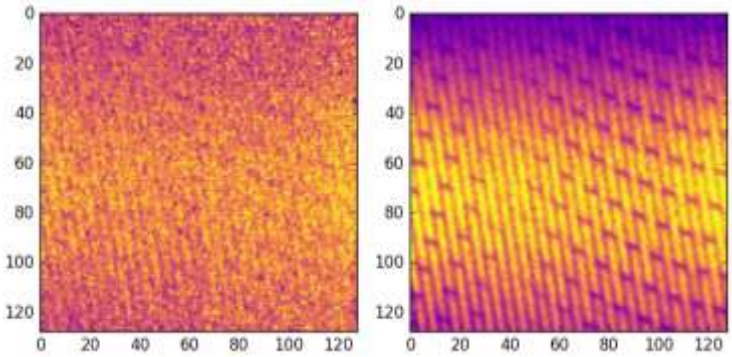

Figure 7. (left) 1000 frame average acquired on the NIT camera at 1000 fps without lock-in. (right) Demodulated 1000 frames modulated by a 113 Hz chopper wheel placed before the gas cell.

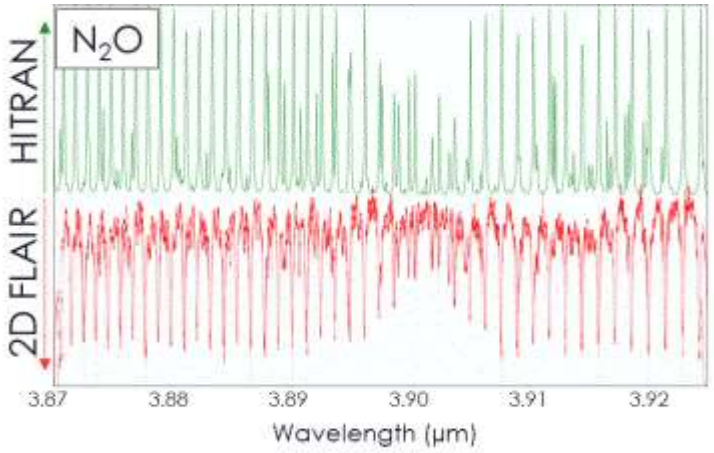

Figure 8. (green) HITRAN database for N_2O (0.1 atm, 10 cm path length). (red) FLAIR measurement of the N_2O reference cell, inversed for clarity. Please notice the low SNR.

Such a spectrum, in the case of the N_2O reference cell, is displayed on the bottom part of Figure 8. Comparison with the HITRAN database simulation indicates a single-shot spectral coverage of 35 cm^{-1} and a sub-nanometer resolution of 0.1 cm^{-1} (corresponding to approx. 3 GHz).

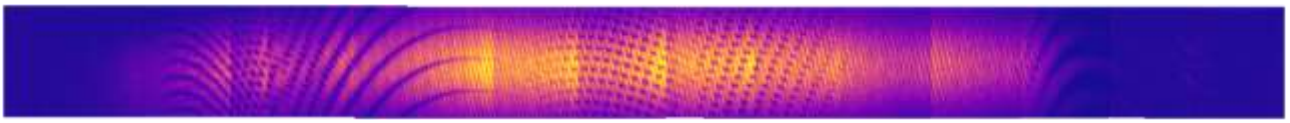

Figure 9. Concatenation of different absorption spectra obtained by tuning laterally the OAP imaging mirror, effectively scanning through a region covering 3.8 to 4.5 µm. The N_2O absorption form a reference cell is visible from the left of the picture to the middle part. The structure on the right corresponds to CO2 present in the air.

Increasing the spectral coverage can be obtained by laterally tuning the position of the imaging OAP. Figure 9 shows the result of several concatenated images acquired by the NIT camera covering the transmission region of the bandpass filter (*i.e.*, from 3.8 to 4.5µm). The absorption structure for the N_2O reference cell is visible on the left portion of othe image. The structure appearing on the right side corresponds to CO_2 present in the laboratory air.

However, the SNR of the signal is rather low, even for highly concentrated gases. Additional tests lead to the conclusion that, e.g., for methane, with a 10 m long MPC, the detection limit would be higher than 5000 ppm, which is incompatible with atmospheric measurements. The current average atmospheric concentration for methane is around 2 to 3 ppm.

We tried different 2D spectrometer approaches, including replacing the VIPA with an Echelle grating or a prism, but without better results on the spectral coverage, resolution, and detection limit.

2.5 1.5D spectrometer (laboratory + flying prototype)

Aiming at increasing the SNR of the signal on the camera, we decided to use a single diffractive element. The schematic principle of the spectrometer design is illustrated on Figure 10. The supercontinuum light goes through a gas cell (or the MPC). The light is then collimated towards the grating. A second OAP images the dispersed light on the camera.

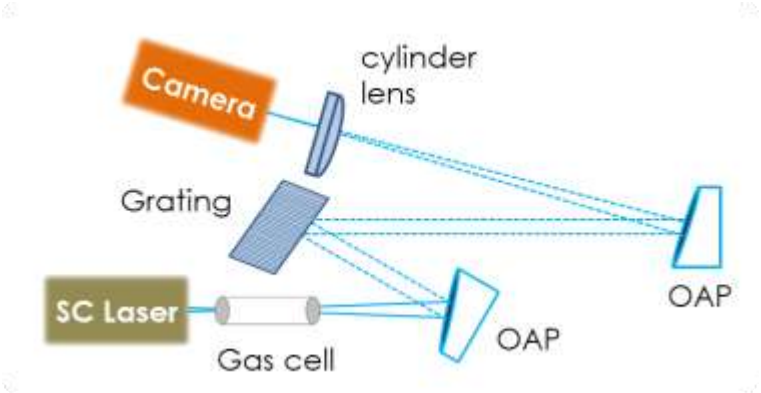

Figure 10. Working principle of the 1.5D spectrometer design used on the final FLAIR prototype. The grating disperses the light in the horizontal direction, and the cylinder lens spreads the spectrum vertically on the 2D matrix detector of the camera. Vertical averaging leads to an increased SNR.

A cylindrical lens spreads the light in the orthogonal direction, resulting in several copies of the spectrum vertically across the matrix detector of the camera. The benefit of this technique on the SNR is readily visible on Figure 11. The violet spectrum corresponds to the situation displayed in the left panel, and the orange spectrum to the one on the right panel, where the vertical spread is increased. The noise on the base of the absorption signal is greatly reduced in the second case. In addition, non-uniformity correction (NUC), this scheme allows to effectively reduce the effect of fixed pattern noise, which is the difference in gain and offset among pixels, typical of mid-IR detectors. Together with the lock-in detection presented in the previous section, the spectrometer has been able to measure sub-ppm levels of methane under laboratory conditions.

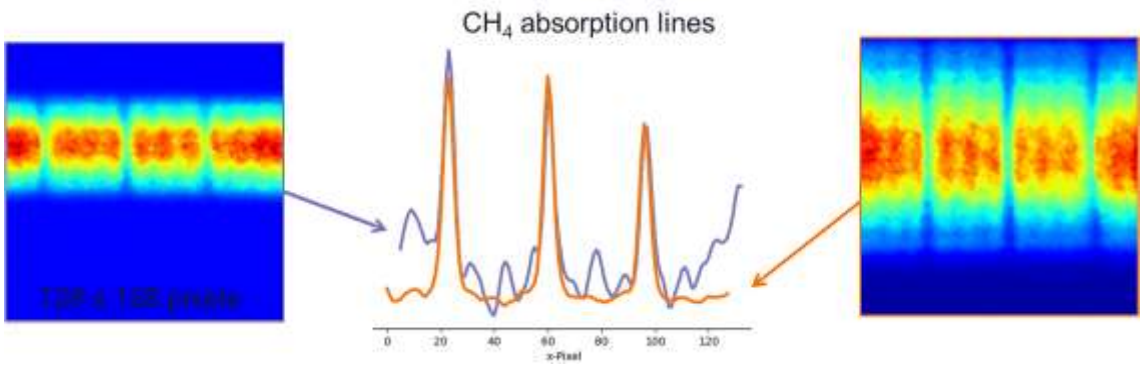

Figure 11. Effect of the cylindrical lens spreading the spectrum vertically on the camera. The violet spectrum corresponds to the situation displayed in the left panel, and the orange spectrum to the one on the right panel, where the vertical spread is increased. The noise on the base of the absorption signal is greatly reduced in the second case.

Figure 12 shows the CAD design of the final spectrometer, and the different elements are listed on the figure. The chopper wheel (2) is placed at the exit of the relfective collimator (1) the supercontinuum is attached to. The collimated beam is then focussed towards the entrance of the MPC(7) by an off axis parabolic mirror (OAP 5). Flat mirros (3, 4, and 6) allow to precisely align the beam toward the entrance of the MPC. After bouncing back-and-forth 40 times, a copy of the entrance beam exits the MPC and is directed by a flat mirror (8) towards the same model OAP(9) as OAP(5). The collimated beam diameter has been calculated to cover as much of the diffraction grating (10) lines, as to reach the required dispersion resolution. The grating is glued to a mototized rotatino platform to cover different wavelenght regions of the SC spectrum. A third OAP (11) images the dispersed light onto the NIT camera (14). The cylindrical lens(13) mentionned in the previous paragraph is placed just bofore the camera. The flat mirror (12) allows to fold the system in order ot keep a compact design. The fabricated prototype is visibel on Figure 16.

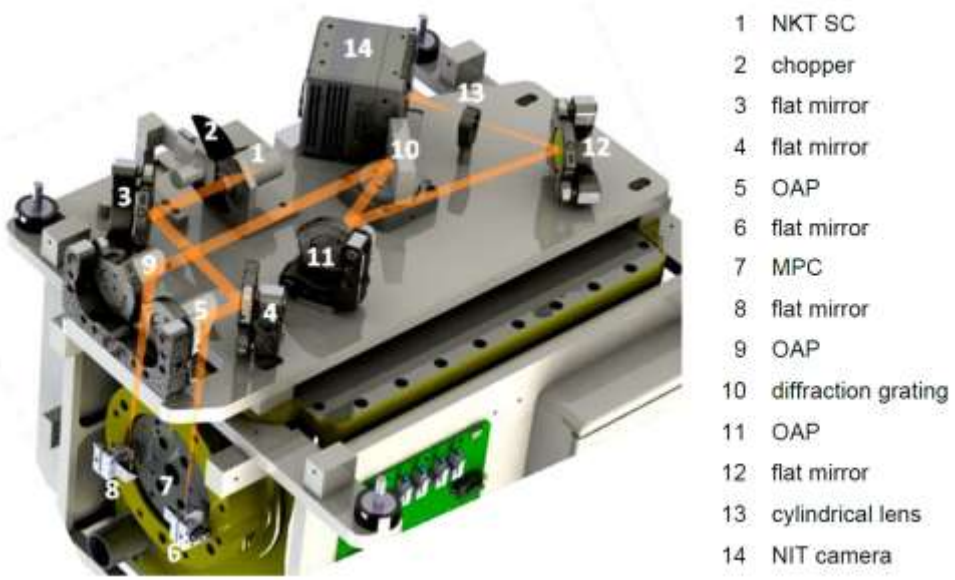

Figure 12. CAD design of the 1.5D spectrometer integrated on top of the multipass cell. The mechanical part linking the spectrometer and the MPC has been removed for better viewing the optical path taken by the SC light.

A dedicated gas handling system has been developped to characterize the FLAIR spectormeter prototype. It consist of a bottle of dry nitrogen, and bottles of methane with concentration 4% and 50 ppm. Mass flow controllers allow to set the desired concentration within the multipass cell. The flow rate is limited to 0.8 Liters per minute.

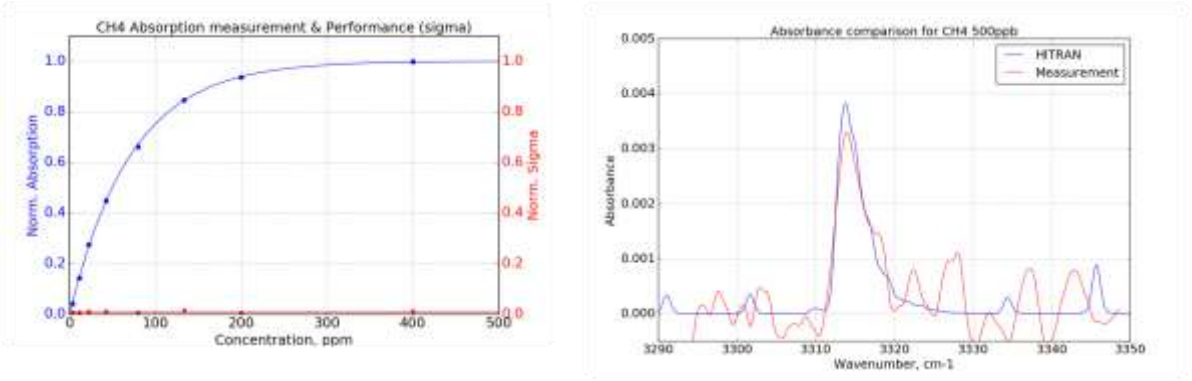

Figure 13. (left) Blue dots are the absorption measured by FLAIR with respect to the methane concentration. The blue line is the calculated Beer Lambert Law. The red line, which is below 0.008 shows the excellent repetability of the measurement. (right) The methane within the MPC has been diluted to 0.5 ppm. The red line is the measured absorption spectrum on the Q-Branch of methane. The blue line is the HITRAN model.

Figure 13 shows some measurement results on different concentration. The FLAIR system follows really well the Beer Lambert law, hence demonstrating its linearity. Moreover, the measurements have been repeated serveral time, and the statistical error remains below 0.008 (normalized sigma). The limit of detection of the FLAIR spectometer is demonstrated on the right panel. Methane with a concentration of 0.5 ppm in dry nitrogen has been flown through the multipass cell. The system has been tuned to detect the intense Q-Branch (at 3315 cm^{-1}). The blue curve shows the model spectrum from the HITRAN database, and the red is the absorbance measured by FLAIR.

Figure 14 shows a real time measurement. Before this experiment, a reference spectrum had been acquired in pure nitrogen. This allows to calculate the real concentration in the MPC. The system has then been under normal atmosphere. There FLAIR detects an ambiant value of 2 ppm for methane, and 1.2% for water concentration, which is consistent with normal laboratory conditions. At minute 2, the gas handling system has been connected, and 50 ppm methane started flowing through the MPC at a flow rate of 0.8L/minute. This can be followed both in the increase of the measured methane level and in the decrease of water vapor concentration. The system slowly reaches equilibrium around 50 ppm methane, as expected. The gas handling system has then been unplugged, and the pumping system started. The measured levels match laboratory atmosphere within a few seconds.

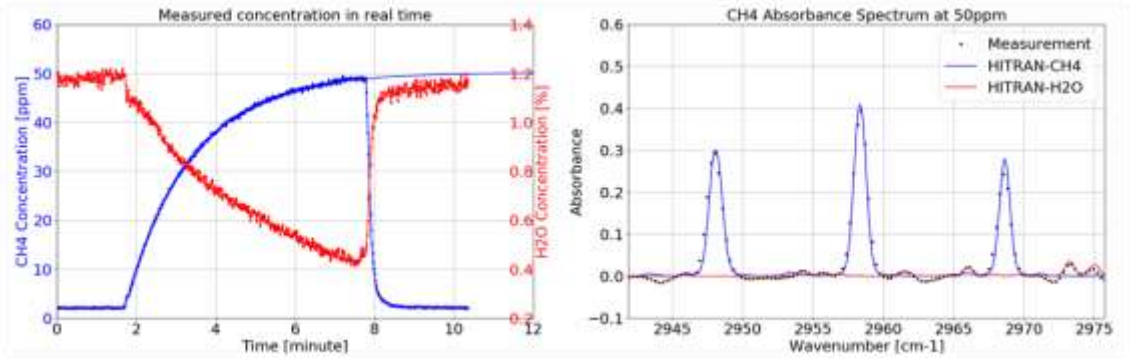

Figure 14. (left) The FLAIR system has been plugged to the gas handling system, and methane with a concentration of 50 ppm has been passed through the system (0.8L/min). At minute 8 the gas handling has been unplugged. In blue, the measured methane concentration, and in red, the spectroscopically measured water concentration. (right) Absorption spectrum for 50 ppm absorption. The black dots are the measured spectrum, the blue curve and the red curve are fitted HITRAN models for methane and water vapor, respectively.

The left pannel shows the detail of the spectrum acquired by FLAIR just before deconnecting the gas handling system (black dots). The corresponding HITRAN simulation for methane and water vapor are visible in blue and red, respectively. The attentive reader has noticed that we did not tune the spectrometer to the Q-Branch of methan, but rather to some of the lower intensity peaks at lower wavenumbers. The reason is that there is a strong overlapping with water vapor at the location of the Q-Branch, which would impair correct estimation in real world condition. In the selected region, however, there are only weak absorption lines for water, which helps the concentration calculation algorithms.

Figure 14 also allows to estimate a single shot spectral coverage 33.9 cm^{-1} and a resolution of 0.7cm^{-1} (equivalent to 21 GHz). The coverage is very similar to the 2D spectrometer prototype, and even though the resolution is reduced by a factor 7, it is still sufficient to efficiently discreminate between different gas absorption lines.

2.6 Real-time concentration measurement algorithm

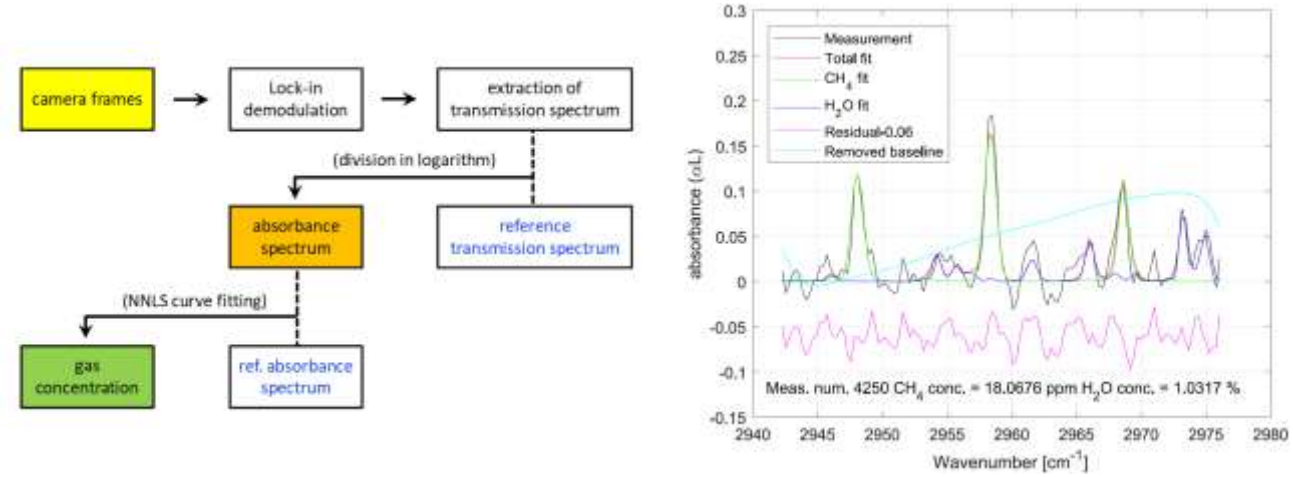

Figure 15. (left) The FLAIR real-time gas concentration measurement algorithm (right) Example of the NNLS curve fitting on measurement performed on the fumes of a LNG propelled ship over open sea.

The camera has been set to acquire 128 x 128 pixels frames at 1000 fps. A LabVIEW program takes care of the camera management, and transfers 1000 images packages to a Python program each second, while managing the following 1000 images acquisition. During this time, the Python program performs the lock-in demodulation using an adaptive frequency detection to compensate for possible drift on the 113 Hz chopper wheel. It then averages the pixel rows to obtain a linear absorption spectrum and stores it on the computer drive for further possible post-processing. The data is then compared to a reference spectrum (logarithm division) to generate the absorbance spectrum. Non-negative least square (NNLS) curve fitting is then applied for concentration estimation, based on pre-defined HITRAN database species of interest. The Python program sheds the results of the analysis back to the LabVIEW interface for real-time display and saves them on the computer hard drive for later processing.

3. SENSOR ASSEMBLY

The design of the sensor and the testing of the sub-systems have been made in parallel during the whole duration of the FLAIR project. Since TEKEVER, the company providing the Unmanned Aerial Vehicle (UAV / drone), had to leave the project, it has been decided to build a compact, and easily transportable system. This would not have been the preferred solution for fitting in a drone since the weight has to be carefully balanced evenly across the whole aircraft.

The fully functional and assembled system is show on Figure 16: the spectrometer part (on top) and the multipass cell are clearly recognizable. On the left picture, one can see the power distribution PCB. It accepts DC voltages from 9 to 36 volts DC to easily adapt different operation condition: 24V laboratory power supply, 12V operation (battery, car cigarette lighter), and 28V (helicopter, UAVs). The different subsystems are connected to different relays that can be programmatically switched on or off. It also provides the 200 kHz trigger for the supercontinuum. Next to it, the fan less

industrial computer on which runs the LabVIEW GUI and the Python program. It runs on Windows 10 and can be remotely accessed to monitor and control the system. During remote operation, a 4G network dongle is attached to the computer.

Figure 16. (left) The FLAIR real-time gas concentration measurement algorithm (right) Example of the NNLS curve fitting on measurement performed on the fumes of a LNG propelled ship over open sea.

The picture on the right shows the other side of the system. In green, the TEC controller to stabilize the temperature of the camera, and a LCD screen to display relevant information on the system without needing to connect to the board computer. The grey box underneath is the driver for the rotation platform onto which the dispersion grating is glued. The black box is the supercontinuum prototype from NKT. Finally, the vertical link ensuring excellent mechanical stability between the spectrometer and the MPC is visible.

During operation, the system is covered by a 3D printed enclosure, to protect the optical elements from dust and debris, keep a relatively constant temperature on the optics, and prevent straylight reaching the eyes of a passerby.

4. VALIDATION CAMPAIGNS

Since the departure of the drone provider from the project team, alternative validation campaigns had to be organized. The maiden flight of FLAIR has been made on a type of zeppelin, formally a thermal airship since it relies on a hot air envelope for buoyancy and not on a lighter than air gas like He or H_2. The zeppelin has been flying over an artificial methane release.

The second campaign has been made onboard a helicopter over the Kattegat channel, linking the North Sea and the Baltic Sea, and measuring the exhaust of 123 ships cruising the channel over 3 days.

4.1 Zeppelin flight over artificial methane release

We performed the first field campaign at the airfield in Beromünster (Switzerland). The instrument was mounted on a hot air zeppelin and operated during a test flight. Methane was released in a controlled way from a gas cylinder (4% concentration) for simulating a significant methane source. The zeppelin flew several times through the plume of the artificial methane source. Figure 17 (left) shows a view of the test site. The FLAIR system is installed on the passenger seat, behind the pilot, and is operated remotely through the 4G datalink. The air intake system, constituted of the blower and a filter, is hanging approximately 2 in front and underneath the cockpit.

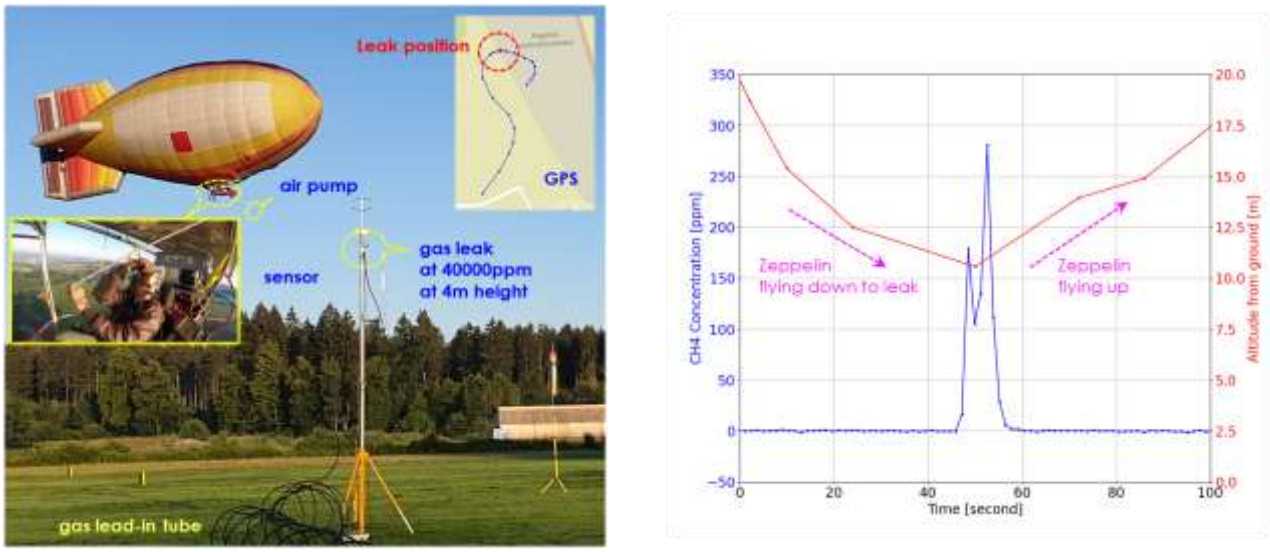

Figure 17. (left) The FLAIR system onboard a zeppelin is flying above an artificial gas leak. (right) Example of a flyby and the measured methane concentration.

The right panel shows, in red, the altitude of the zeppelin, and in blue the retrieved methane concentration of one of the flybys.

Thus, the capabilities of the FLAIR instrument for detecting elevated methane concentration were demonstrated. This first field campaign showed that the FLAIR instrument can successfully be operated on an airborne platform. The field tests provided valuable experience and information for the second planned field campaign.

4.2 Helicopter campaign over ship exhaust plumes

The second field test of the FLAIR instrument has been performed in Denmark in collaboration with Explicit ApS on a helicopter operated by Charlie9 Helicopters ApS. The flights took place for 3 days and allowed the observation of 123 ship plumes. In addition to a CO2, NOx, SOx, and particles sensor, Explicit was using a commercial sensor specifically for methane detection (LGD Compact-A CH4 from Axetris). This was a good opportunity to benchmark our system.

The FLAIR system has been installed on the rear passenger seat, and the air intake extended to the front of the helicopter, near the air intake of the commercial reference system (Figure 18A). The FLAIR team stayed on ground and monitored the system remotely. On several occasion, the 4G network has been lost, as the helicopter was flying away from the coastline and at low altitude. The system was nevertheless robust enough to continue operation on a standalone way.

The helicopter would take off from Roskilde airport, near Copenhagen, and fly toward the north of Denmark where it lands for refueling. It then flies back in the afternoon. On its way, it targets the ships cruising the Kattegat channel (colored squares on Figure 18B) and flies directly into the plumes of the exhaust of the ship (Figure 18C). The measurement relies on the experience of the pilot, and on the reading of the CO_2 detector, which the pilot tries to maximize. It stays around 1 minute inside the plume.

Among the 123 ships measured during these 3 days campaign, only 3 showed methane release in their plumes. An LNG tanker, a cruise ship, and a container cargo ship. All three had engines running on LNG (Liquefied Natural Gas). For each of those 3 ships, the helicopter did several flybys into the plumes. Figure 18D shows, in red, the retrieved methane concentration on ship #22. Before flying into the plume, the methane level is at atmospheric values. Once in the plume, it reaches approximately 18 ppm. The grey traces show the measurement result of the commercial system. Both traces match almost perfectly. This is particularly striking on the zoom of the first flyby.

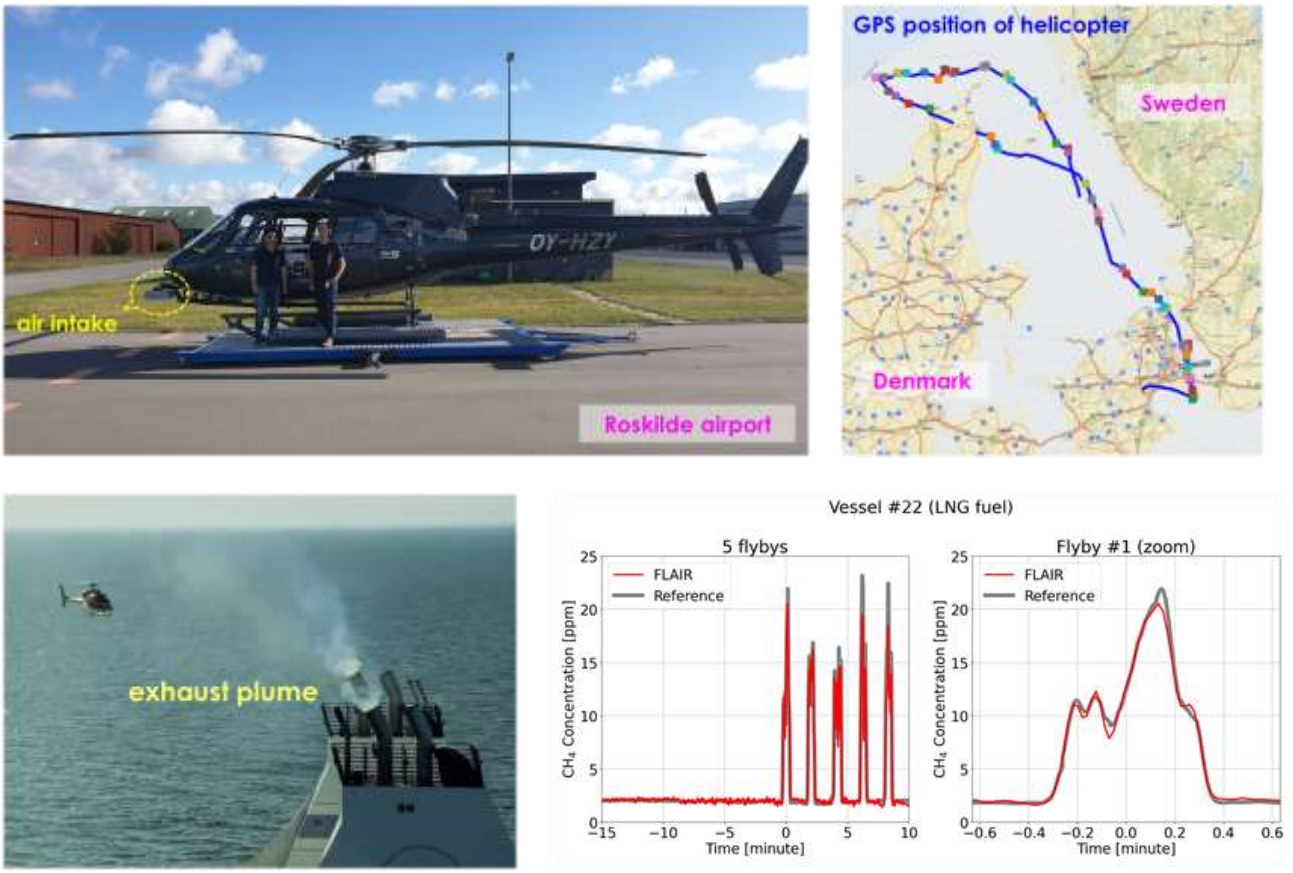

Figure 18. (left) The FLAIR system onboard a zeppelin is flying above an artificial gas leak. (right) Example of a flyby and the measured methane concentration.

5. CONCLUSION

The FLAIR team successfully designed, assembled, and tested a compact airborne-compatible spectrometer, with a volume of 55 Liters, a weight of 16 kg and around 80W power consumption. The system can operate standalone and be monitored remotely thanks to a 4G datalink. It performs one measurement per second and has a 0.7 cm^{-1} spectral resolution over 38 cm^{-1} range for a single shot measurement. The detection window is tunable to match different species of interest. The sensitivity is sufficient to reach the atmospheric background level for methane.

We demonstrated its capabilities during laboratory tests, but above all on 2 airborne campaigns. The first one onboard a zeppelin to measure simulated methane leak, and the second one onboard a helicopter to measure the air quality emitted by ships cruising the seas. A comparison with commercial reference systems confirmed that CH_4 and H_2O vapor were measured accurately.

6. ACKNOWLEDGEMENT

The project underlying this paper has received funding from the European Union's Horizon 2020 research and innovation program under Grant Agreement No 732968 (FLAIR). The authors are also thankful to P. Galley and F. Droz from Bluesky Ballooning, T. Jans from Charlie9 Helicopters, and B. Knudsen, J. Knudsen, and S. Jørgensen from Explicit AS who made the airborne campaigns possible.

7. ADDITIONAL MATERIAL

More information on FLAIR can be found on the project webpage: https://www.h2020flair.eu/

The project team produced 2 documentaries recounting the history and results of FLAIR:

The Flying Grand Piano (https://vimeo.com/507077454)

The Dog & the Eagle (https://vimeo.com/291061243)

REFERENCES

[1] Eslami Jahromi, K., Pan, Q., Khodabakhsh, A., Sikkens, C., Assman, P., Cristescu, S., Moselund, P., Janssens, M., Verlinden, B., Harren, F., "A Broadband Mid-Infrared Trace Gas Sensor Using Supercontinuum Light Source: Applications for Real-Time Quality Control for Fruit Storage." Sensors. 2019; 19(10):2334. https://doi.org/10.3390/s19102334

[2] Kubat, I., Agger, C., Moselund, P., and Bang, O., "Mid-infrared supercontinuum generation to 4.5 μm in uniform and tapered ZBLAN step-index fibers by direct pumping at 1064 or 1550 nm," J. Opt. Soc. Am. B 30, 2743-2757 (2013).

[3] Petersen, C., Moselund, P., Huot, L., Hooper, L., and Bang, O., "Towards a table-top synchrotron based on supercontinuum generation", Infrared Physics & Technology 91, 182-186 (2018), https://doi.org/10.1016/j.infrared.2018.04.008

[4] Méndez-Rial, R., Souto-López, Á., Rodríguez-García, J., Rodríguez-Araújo, J., and García-Díaz, A. "A high-speed MWIR uncooled multi-aperture snapshot spectral imager for IR surveillance and monitoring." 2016 IEEE International Conference on Imaging Systems and Techniques (IST), 206-210. (2016).

[5] Nugent-Glandorf, L., Neely, T., Adler, F., Fleisher, A., Cossel, C., Bjork, B., Dinneen, T., Ye, J., and Diddams, S., "Mid-infrared virtually imaged phased array spectrometer for rapid and broadband trace gas detection," Opt. Lett. 37, 3285-3287 (2012)